PHYSICAL REVIEW B VOLUME 57, NUMBER 9 1 MARCH 1998-I

Effect of OH content on the far-infrared absorption and low-energy states in silica glass

T. Ohsaka and S. Oshikawa
Research Institute for Scientific Measurements, Tohoku University, Katahira, Aoba-ku, Sendai 980, Japan

(Received 5 September 1997)

The far-infrared absorption for two types of silica glasses (containing $\leqslant 1$ ppm and ~ 200 ppm of OH) has been quantitatively investigated in the region $10-100\ \mathrm{cm}^{-1}$ at room temperature. An absorption coefficient $\alpha(\nu)$ increased with increasing OH content and a broad peak on a plot of $\alpha(\nu)/\nu^2$ vs ν, corresponding to a ''boson peak'' shifted from 41 to $36\ \mathrm{cm}^{-1}$. The OH-related absorption increase $\Delta\alpha(\nu)$, showed a monotonic increase with frequency ν in contrast to that previously published. The rate of the absorption increase $\Delta\alpha(\nu)/\alpha(\nu)$ showed a rapid decrease with frequency obeying a power-law $\propto \nu^{-1.7}$ between ~ 17 and $51\ \mathrm{cm}^{-1}$, whereas it decreased very slowly below $\sim 17\ \mathrm{cm}^{-1}$. It is suggested on the basis of a noncontinuous network model for the glass that OH ions are not uniformly distributed in silica glass. The light-vibration coupling coefficient determined experimentally is briefly discussed by some models proposed before.

[S0163-1829(98)03009-4]

It is well known that glasses exhibit physical properties significantly different from crystalline solids, particularly in the low-energy region $1 \sim 10$ meV, for example, the excess of the low-frequency vibration density of states (VDOS) not described by the Debye approximation, low-temperature excess heat capacity, plateau in low-temperature thermal conductivity, low-frequency light scattering, far-infrared (FIR) absorption, etc.[1,2] These anomalous and universal properties are thought to be related to intermediate range order in glasses, but its origin is not yet clear. Silica glass is the most representative and probably most widely studied glass in amorphous solids. The low-energy properties in silica glass, and the effects of OH content on bulk properties such as dielectric constant, refractive index, density, elastic behavior, and thermal conductivity have also been studied.[3–5] Water in silica glass plays an important role and is associated with differences in physical and structural properties.

Although the FIR absorption measurements on silica glass have been extensively made,[2,6–8] there are still discrepancies as to the frequency ν dependence of absorption coefficients $\alpha(\nu)$, in particular in the low-frequency region below $\sim 30\ \mathrm{cm}^{-1}$, and as to peak values in $\alpha(\nu)/\nu^2$ vs ν plot, corresponding to ''boson peaks.'' Stolen[2] measured FIR absorption and low-frequency Raman scattering in SiO_2, GeO_2, and B_2O_3 glasses, and indicated a similarity between the FIR absorption and Raman scattering in glasses. Hutt and co-workers[6] measured the FIR absorption on Spectrosil WF (a few ppm of OH) and Spectrosil B (~ 1200 ppm of OH) at room temperature, 200 K, and 80 K using a FIR laser at intervals between 20 and $100\ \mathrm{cm}^{-1}$ (see Fig. 1, where open squares are for Spectrosil WF, plus signs for Spectrosil B). They found that the FIR absorption of Spectrosil WF was independent of temperature, and the existence of OH in silica glass increased the FIR absorption. They furthermore reported that this OH-related FIR absorption decreases with decreasing temperature. Ahmad[9] showed a similarity between frequency dependencies of both the FIR and Raman coupling coefficients between light and low-frequency vibrations in silica glass. In this work we report results of FIR absorption measurements on two types of silica glasses with different OH contents. The purpose is to provide more accurate absorption data on silica glass, to assess quantitatively an OH contribution to the FIR absorption, and to consider the experimentally obtained frequency dependence of the coupling coefficient between the FIR light and the low-energy states.

Experiments were carried out on two types of commercially available silica glasses with different OH contents, T-2020 (called A) and T-1020 (called B), trademarks of Toshiba Ceramics Co. Ltd. Disk-shaped samples of each type of silica glass were cut from each ingot and both surfaces were polished optically flat with diamond paste. For absorption measurements several plane parallel slabs of 15 mm diameter were used ranging in thickness from about 0.5 to 5 mm depending on absorption strength. The thickness of the samples was determined with an accuracy of $\pm 1.5\ \mu$m using a micron-micrometer. OH contents in the glass samples were obtained from measurements of absorbance of the infrared band at about $3675\ \mathrm{cm}^{-1}$ due to the OH-stretching vibration.[4] The OH content was about $\leqslant 1$ ppm (below the detecting limit of an infrared spectrometer) for glass A and about 200 ppm for glass B. FIR absorption measurements were made with a Martin-Puplett-type Fourier transform spectrometer[10] in the range $10-100\ \mathrm{cm}^{-1}$ at room temperature. A liquid-He cooled Si-composite bolometer was used as a detector. The FIR absorption coefficient was determined from the transmission through a plane parallel slab using the usual expression for normal incidence,

$$T=\frac{(1-R)^2 e^{-\alpha d}}{(1-Re^{-\alpha d})^2+4Re^{-\alpha d}\sin^2(2\pi n\nu d)},$$

which includes the effect of multiple reflections within the parallel slab. α is the absorption coefficient, d the thickness, n the refractive index, and $R \approx (n-1)^2/(n+1)^2$ a single surface reflectivity at normal incidence. n was determined from interference maxima[11] in interference-fringe transmission spectra of thin samples of approximately 0.5 and 1 mm in

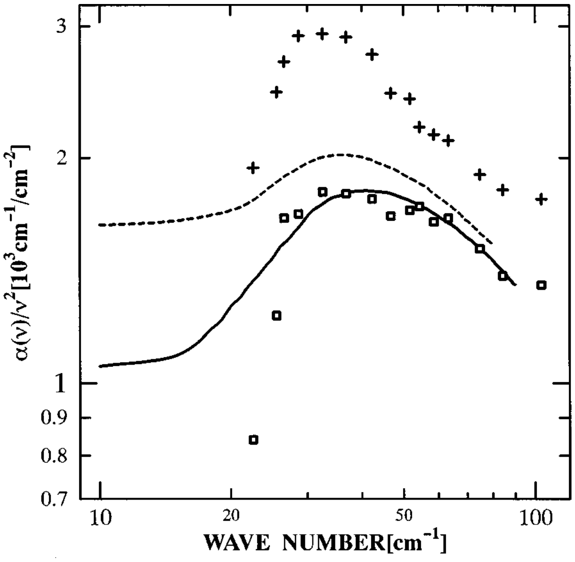

FIG. 1. Comparison of far-infrared absorption coefficients $\alpha(\nu)$ in silica glasses with different OH contents at room temperature on a log-log plot of $\alpha(\nu)/\nu^2$ vs ν. The solid curve, glass A ($\sim$1 ppm of OH); the dashed curve, glass B ($\sim$200 ppm of OH); open squares, Spectrosil WF (a few ppm of OH) taken from Ref. 6; plus signs, Spectrosil B ($\sim$1200 ppm of OH) taken from Ref. 6.

thickness. For example, $n=1.951\pm0.002$ at 30 cm^{-1} for glass A. The reflectivity was evaluated from n determined in the above manner.

Figure 1 compares the obtained room-temperature absorption coefficients $\alpha_A(\nu)$ in the solid curve for glass A and $\alpha_B(\nu)$ in the dashed curve for glass B on a log-log plot of $\alpha(\nu)/\nu^2$ vs ν together with the FIR data by Hutt and co-workers.[6] In this figure, $\alpha(\nu)/\nu^2$ in glass A shows a very slow increase with frequency, a steep rise near 15.5 cm^{-1}, and then a broad peak at about 41 cm^{-1}, corresponding to the boson peak. Glass B also shows similar behavior. Our absorption data on glass A are close to the data on Specrosil WF by Hutt and co-workers[6] for frequencies above $\sim$30 cm^{-1}, but there are discrepancies below $\sim$30 cm^{-1}. It is evidently found from this figure that the introduction of OH into silica glass increases the overall FIR absorption, and furthermore shifts the broad peak to the lower frequency side from 41 cm^{-1} (glass A) to 36 cm^{-1} (glass B). Figure 2 shows the OH-related absorption increase $\Delta\alpha(\nu)=\alpha_B(\nu)-\alpha_A(\nu)$ in the dashed curve, and the rate of the absorption increase $\Delta\alpha(\nu)/\alpha_A(\nu)$ in the solid curve as a function of frequency on a log-log plot. The absorption increase $\Delta\alpha(\nu)$ increases monotonically with frequency in contrast to the result[12] previously reported, in which $\Delta\alpha(\nu)$ shows a peak at about 30 cm^{-1}. On the other hand, the rate of the absorption increase $\Delta\alpha(\nu)/\alpha_A(\nu)$ shows an abrupt transition near 17 cm^{-1}, and a peculiar frequency dependence: $\Delta\alpha(\nu)/\alpha_A(\nu)$ decreases rapidly with frequency obeying a power-law like $\propto\nu^{-1.7}$ (the dotted line in Fig. 2) between $\sim$17 and 51 cm^{-1}. This frequency range corresponds just to the boson peak. This power-law frequency dependence of the effect of OH on the FIR absorption has not previously been observed. For frequencies below $\sim$17 cm^{-1}, $\Delta\alpha(\nu)/\alpha_A(\nu)$ shows a very slow decrease with frequency.

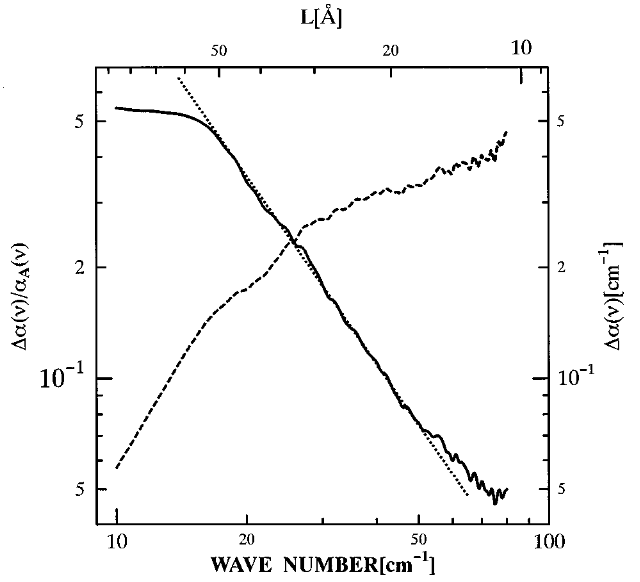

FIG. 2. OH-related absorption increase, $\Delta\alpha(\nu)=\alpha_B(\nu)-\alpha_A(\nu)$ (dashed curve), and the rate of the absorption increase, $\Delta\alpha(\nu)/\alpha_A(\nu)$ (solid curve) as a function of frequency in silica glass on a log-log plot. The dotted line shows a power-law frequency dependence $\Delta\alpha(\nu)/\alpha_A(\nu)\propto\nu^{-1.7}$ between 17 and 51 cm^{-1}. The upper abscissa is expressed in cluster size L(Å). See the text.

Generally, the FIR absorption coefficient $\alpha(\nu)$ of glasses or amorphous solids is expressed in the following equation:[13]

$$\alpha(\nu)=C(\nu)g(\nu),$$

where $g(\nu)$ is VDOS, and $C(\nu)$ the coupling coefficient between FIR light and vibrations. Now we assume that when water is introduced into silica glass the frequency dependence of the coupling coefficient $C(\nu)$ is unchanged, although the absolute values of the coupling coefficient might change. Then, $\Delta\alpha(\nu)/\alpha_A(\nu)\approx\Delta g(\nu)/g(\nu)$. Here, $\Delta g(\nu)=g_B(\nu)-g_A(\nu)$ is a change of VDOS. The above relation means that the rate of absorption increase corresponds to the rate of the VDOS change. The VDOS change $\Delta g(\nu)$ is obtained as $\Delta g(\nu)\approx g(\nu)\Delta\alpha(\nu)/\alpha_A(\nu)$. Furthermore, a frequency distribution of the total number of modes with the frequency below ν, which occur newly by the introduction of OH, $\Delta N(\nu)$, is given as follows: $\Delta N(\nu)\approx\int_0^\nu\Delta g(\nu)d\nu$. Thus, $\Delta g(\nu)$ and $\Delta N(\nu)$ were evaluated using the absorption coefficients obtained here and VDOS (Ref. 14) determined from inelastic neutron scattering.

Figure 3 shows $\Delta g(\nu)$ (the dashed curve) and $\Delta N(\nu)$ (the solid curve) calculated in the above manner. $\Delta g(\nu)$ rises slowly with frequency, shows a broad peak around 45 cm^{-1}, and then decreases slowly. $\Delta N(\nu)$ increases with frequency, but appears to have two inflection points near 18 and 39 cm^{-1}. This behavior of $\Delta N(\nu)$ is similar to that of $\Delta\alpha(\nu)/\alpha_A(\nu)$ or $\Delta g(\nu)/g(\nu)$. In Fig. 3 the dotted line shows $\Delta N(\nu)\propto\nu^{2.5}$. Since $\Delta N(\nu)$ is the total number of new modes with frequency below ν, which occur by the addition of OH into silica glass, the frequency distribution of the new modes shows the power-law frequency dependence $\Delta N(\nu)\propto\nu^{2.5}$ between 18 and 39 cm^{-1}. This might mean that the

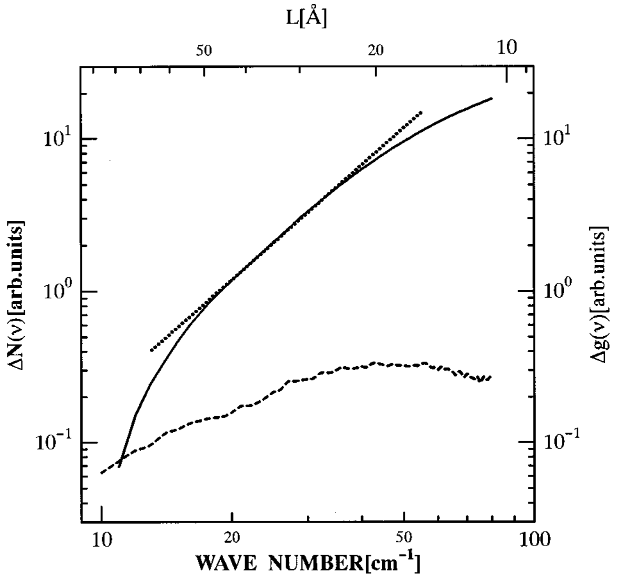

FIG. 3. OH-related increase of VDOS, $\Delta g(\nu)$ (dashed curve), and the frequency distribution of the total number of OH-related new modes with the frequency below ν, $\Delta N(\nu)$ (solid curve) as a function of frequency in silica glass on a log-log plot. The dotted line shows a power-law frequency dependence $\Delta N(\nu) \propto \nu^{2.5}$ between 18 and 39 cm^{-1}. The upper abscissa is expressed in cluster size L(Å). See the text.

frequency distribution of the new modes is fractal-like with the fractal dimension of 2.5 in the frequency range 18–39 cm^{-1}.

Achibat and co-workers[15] showed from the temperature dependence of the low-frequency light scattering in silica glass that the structural relaxation modes have an effect up to 20 cm^{-1} at room temperature. It is suggested from their results and the abrupt transition observed near 17 cm^{-1} in $\Delta\alpha(\nu)/\alpha_A(\nu)$ that below ~17 cm^{-1} the FIR absorption is due partly to relaxation modes besides vibration modes and above ~17 cm^{-1} due to vibration modes. The similar transition was also observed at 20 cm^{-1} in VDOS (Ref. 14) obtained from inelastic neutron scattering, and in the light-vibration coupling coefficient[15] obtained from low-frequency Raman scattering for silica glass. These experimental results were explained well by assuming that the glass network is not continuous, but composed of disordered blobs or clusters.[15,16] The disordered glass network is disrupted by defects which segregate the structure into blobs or clusters. In silica glass OH is a kind of defect, and therefore would play a role in producing blobs or clusters. According to the above model of the noncontinuous random network of glass, it is expected that VDOS in high-frequency vibration region increases as the number of clusters able to accommodate the vibrations increases.

Let us consider the effect of OH on the FIR absorption on the basis of the noncontinuous network model or the cluster model mentioned above. The fundamental vibration mode localized in a cluster has a frequency ν such that[15]

$$\nu = S(k/cL) \quad [\mathrm{cm}^{-1}],$$

where c is the velocity of light, k the velocity of sound, L a cluster size, and S a shape factor below 1. Therefore the size distribution of clusters corresponds to a frequency distribution of the fundamental modes in clusters. Using the above equation, the vibration frequency ν is interchanged into the cluster size L. We choose $S = 0.65$ as Achibat and co-workers[15] did. The upper abscissas of Figs. 2 and 3 are expressed in cluster size L(Å) instead of frequency ν as $S = 0.65$ and $k = 4.00 \times 10^5$ [cm/sec] for silica glass.[15] As seen in Fig. 2, the OH-related absorption increase $\Delta\alpha(L)$ decreases monotonically with cluster size L. On the other hand, the rate of absorption increase $\Delta\alpha(L)/\alpha_A(L)$, increases with cluster size L. Since in the above cluster model the increase of VDOS corresponds to the increase of the number of clusters, Fig. 2 shows the dependence of the increase rate of VDOS or the cluster number on the cluster size L. Figure 2 also shows that the increase rate of the cluster number increases with cluster size L obeying a power-law like $\propto L^{1.7}$ between ~17 and 51 Å, but increases very slowly with L above ~51 Å.

It is also seen from Fig. 3 that the increase of VDOS or the cluster number, $\Delta g(L)$, increases slowly with cluster size, shows a broad peak near 19 Å corresponding to 45 cm^{-1}, and then decreases slowly. The size distribution of total number of clusters with the size above L, $\Delta N(L)$, shows a power-law size dependence $\propto L^{-2.5}$ between ~22 and 48 Å. This size range 22–48 Å corresponds to the frequency range 39–18 cm^{-1}. As mentioned above on the frequency distribution of new modes, this might mean that the size distribution of clusters is fractal-like with the fractal dimension of 2.5 between 22 and 48 Å. Since the size distribution of clusters reflects the space distribution of OH in silica glass, the above result suggests that OH ions are not uniformly distributed.

Next we consider the coupling coefficient between FIR light and vibrations in silica glass. As known from the equation, $\alpha(\nu) = C(\nu)g(\nu)$, the coupling coefficient $C(\nu)$ can be obtained experimentally if $\alpha(\nu)$ and $g(\nu)$ were determined

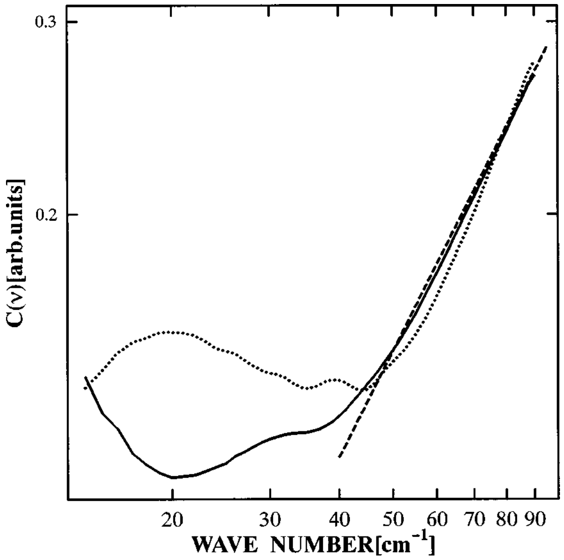

FIG. 4. Far-infrared coupling coefficients $C(\nu)$ obtained using VDOS given by Buchenau *et al.*[17] (solid curve), and by Dianoux[14] (dotted curve) from inelastic neutron scattering. The dashed line shows a linear frequency dependence $C(\nu) \propto \nu^{1.0}$.

experimentally. Fortunately, $g(\nu)$ of silica glass is determined experimentally as mentioned above. Thus, $C(\nu)$ were evaluated using $\alpha(\nu)$ obtained here for glass A, and $g(\nu)$ determined from inelastic neutron scattering. In Fig. 4 the solid curve and the dotted curve show $C(\nu)$ obtained using $g(\nu)$ given by Buchenau *et al.*[17] and by Dianoux,[14] respectively. In this figure the dashed line shows a linear frequency dependence $C(\nu)\propto\nu^{1.0}$. Both the $C(\nu)$ curves show a nearly linear frequency dependence in the frequency side above $\sim 40\ \mathrm{cm}^{-1}$. However they show the deviation from it in the lower-frequency side, although there is seen the discrepancy between them.

No microscopic theory or model for the FIR coupling coefficient in glasses or amorphous solids presently exist. In a soft-potential model,[18] $C(\nu)$ is independent of frequency. Accordingly, $C(\nu)$ obtained here experimentally cannot be explained by this model. According to the Martin-Brenig model,[19] which has been extensively used for the interpretation of Raman scattering of glasses, $C(\nu)$ shows a maximum contrary to that obtained experimentally here. The noncontinuous network model[15,16] mentioned above and also a fractal model[20,21] predict a nearly linear frequency dependence for $C(\nu)$. This prediction is close to the behavior of $C(\nu)$ obtained here above $\sim 40\ \mathrm{cm}^{-1}$. However we cannot yet explain satisfactorily the frequency dependence of the light-vibration coupling coefficient in the low-frequency region in glasses.

In summary, OH in silica glass increased the FIR absorption and shifted the peak corresponding to the boson peak to the lower-frequency side. The OH-related absorption increase $\Delta\alpha(\nu)$, increased monotonically with frequency. The rate of the absorption increase $\Delta\alpha(\nu)/\alpha_A(\nu)$, decreased rapidly obeying the power-law frequency dependence $\propto\nu^{-1.7}$ between ~ 17 and $51\ \mathrm{cm}^{-1}$, and below $\sim 17\ \mathrm{cm}^{-1}$ showed the very slow decrease with frequency. This abrupt transition observed in $\Delta\alpha(\nu)/\alpha_A(\nu)$ between the two frequency regions at $\sim 17\ \mathrm{cm}^{-1}$ suggested that the high-frequency modes above $\sim 17\ \mathrm{cm}^{-1}$ are vibrational, whereas in the lower-frequency region there exist the relaxation modes. It was suggested on the basis of the noncontinuous network model that the OH-distribution is not uniform in silica glass. It was found that the FIR light-vibration coupling coefficient determined experimentally is not explained by the soft-potential model, and also the Martin-Brenig model, but the nearly linear frequency dependence above $\sim 40\ \mathrm{cm}^{-1}$ is close to the prediction by the noncontinuous network model or the fractal model.

The authors would like to thank Professor M. Ikezawa for his encouragement and valuable discussions during the course of this work, and K. Yanagi for polishing the glass samples. This research was in part supported by a Grant-in-Aid for Scientific Research from the Ministry of Education, Science, and Culture of Japan.

---

[1] *Amorphous Solids: Low Temperature Properties*, edited by W.A. Phillips (Springer-Verlag, Berlin, 1981).

[2] R. H. Stolen, Phys. Chem. Glasses **11**, 83 (1970).

[3] C. Andeen, D. Schuele, and J. Fontanella, J. Appl. Phys. **45**, 1071 (1974).

[4] G. Hetherington and K. H. Jack, Phys. Chem. Glasses **3**, 129 (1962).

[5] H. Kobayashi, T. Kosugi, and Y. Kogure, Physica B **219&220**, 276 (1996).

[6] K. W. Hutt, W. A. Phillips, and R. J. Butcher, J. Phys.: Condens. Matter **1**, 4767 (1989).

[7] L. Chivelder and W. A. Phillips, J. Non-Cryst. Solids **109**, 280 (1989).

[8] U. Strom and P. C. Taylor, Phys. Rev. B **16**, 5512 (1977).

[9] N. Ahmad, Phys. Rev. B **48**, 13 512 (1993).

[10] T. Ihara and T. Ohsaka, Bull. Res. Ins. Sci. Meas. Tohoku Univ. **42**, 1 (1993).

[11] S. Zzerdling, J. Opt. Soc. Am. **60**, 787 (1970).

[12] R. H. Stolen and G. E. Walrafen, J. Chem. Phys. **64**, 2623 (1976).

[13] F. L. Galeener and P. N. Sen, Phys. Rev. B **17**, 1928 (1978).

[14] A. J. Dianoux, Philos. Mag. B **59**, 17 (1989).

[15] T. Achibat, A. Boukenter, and E. Duval, J. Chem. Phys. **99**, 2046 (1993).

[16] E. Duval, N. Garcia, A. Boukenter, and J. Serughetti, J. Chem. Phys. **99**, 2040 (1993).

[17] U. Buchenau, M. Prager, N. Nucker, A. J. Dianoux, N. Ahmad, and W. A. Phillips, Phys. Rev. B **34**, 5665 (1986).

[18] See, for example, D. A. Parshin, Phys. Solid State **36**, 991 (1994).

[19] A. J. Martin and W. Brenig, Phys. Status Solidi B **64**, 163 (1974).

[20] S. Alexander and R. Orbach, J. Phys. Lett. **43**, 625 (1982).

[21] R. Orbach, J. Stat. Phys. **36**, 735 (1984).